JOURNAL OF SOLID STATE CHEMISTRY 3, 614–620 (1971)

Nonstoichiometric Alkali Ferrites and Aluminates in the Systems $NaFeO_2$–TiO_2, $KFeO_2$–TiO_2, $KAlO_2$–TiO_2, and $KAlO_2$–SiO_2

C. LI, A. F. REID, AND S. SAUNDERS

Division of Mineral Chemistry, CSIRO, P.O. Box 124, Port Melbourne, Victoria 3207, Australia

Received March 2, 1971

Examination of $NaFeO_2$–TiO_2 compositions has shown that the α–$NaFeO_2$ structure can be given a range of nonstoichiometry $Na_{1-x}Fe_{1-x}Ti_xO_2$, $O \leqslant x \leqslant 0.28$. The additional Ti atoms are randomized with Fe atoms, and charge balance is maintained by a partial occupancy of the Na atom layers. Fractional occupancy of alkali ion sites in other compounds in the $NaFeO_2$–TiO_2 system and in the systems $KAlO_2$–TiO_2, $KAlO_2$–SiO_2, and $KFeO_2$–TiO_2 was also found. In TiO_4 tetrahedra, Ti^{4+} was deduced to have a Ti–O bond length of 1.92 Å.

Introduction

The combination of alkali metal oxides with the oxides of trivalent metal ions provides a large number of ABO_2 compounds (*1–3*) of which α-$NaFeO_2$ (*4*), based on the rocksalt structure, and $KFeO_2$ (*5*), based on the cristobalite structure, are typical.

We have found that a number of ABO_2 compounds can incorporate TiO_2 in their structures, and additionally, those based on cristobalite can incorporate SiO_2. The details of the resulting nonstoichiometry and its relationship to that of other nonstoichiometric phases in the ABO_2–TiO_2 systems form the subject of the present paper.

Experimental

Sodium based compositions of the type $Na_{1-x}Fe_{1-x}Ti_xO_2$ were prepared from analytical reagent grade sodium oxalate, and Fisher certified Fe_2O_3 and TiO_2. After thorough grinding, the preparations were heated at 600°C for several hours, and then at 650°C for $x = 0$, 800°C for $x = 0.05$ and 0.10, and at 1000°C for $x > 0.15$. The α form of $NaFeO_2$ is transformed near 760° to a β form (*6–8*) based on the wurtzite structure. In the present work, this transformation temperature was found to be raised above 1000°C by addition of between 10 and 20 mole % TiO_2 to α-$NaFeO_2$ and the temperatures of preparation were chosen to avoid the α–β conversion.

Potassium-based compounds were made from dried potassium carbonate and, variously, Al_2O_3, Fe_2O_3, TiO_2 and precipitated silica. After initial grinding and firing at 900°C, all preparations based on $KAlO_2$ were reground and heated overnight at 900°C. $KFeO_2$ was prepared at 800°C, and $K_{1-x}Fe_{1-x}Ti_xO_2$ compositions at 750°C. The potassium compounds were sensitive to atmospheric moisture, and were cooled and manipulated in a dry atmosphere.

Lithium compounds were made from lithium carbonate dried at 300°C and were heated at a final temperature of 1000°C.

X-Ray Data

X-Ray data were obtained on a powder diffractometer fitted with monochromator and proportional counter. Recordings were made at slow scan rates, and either silicon powder, $a_0 = 5.4301$ Å or potassium chloride, $a_0 = 6.293$ Å, was included as an internal standard. Potassium compounds were protected by an atmosphere of dry nitrogen as it was found that absorption of atmospheric moisture markedly affected the cubic lattice parameter. For the hexagonal compounds, final lattice parameters were obtained by a least squares fit of the observed data. Reflection intensities for $Na_{0.75}Fe_{0.75}Ti_{0.25}O_2$ were obtained from the areas of recorded diffraction peaks.

The lower limit of the narrow fractional occupancy

range for sodium in the $NaFeTiO_4$ structure, 0.970 ± 0.005, was determined by measuring the relative intensities of the $NaFeTiO_4$ (*9*) and $Na_xFe_xTi_{2-x}O_4$ (*10*) powder patterns obtained at several compositions in their region of coexistence, and extrapolating to a zero value for $Na_xFe_xTi_{2-x}O_4$.

Results

The variation in lattice parameters for α-$NaFeO_2$–TiO_2 solid solutions are shown in Fig. 1 and limiting values are given in Table I. It is evident that the composition range $Na_{1-x}Fe_{1-x}Ti_xO_2$, exists with $0 \leqslant x \leqslant 0.28$. Beyond this concentration, the lattice parameters remained constant, and $NaFeTiO_4$ (*9*), the next phase in the pseudobinary $NaFeO_2$–TiO_2 system, began to appear.

Structure factor calculations for $Na_{0.75}Fe_{0.75}Ti_{0.25}O_2$ were made after converting the observed intensities to structure factors, with appropriate allowance for multiplicity and Lorentz polarization. Calculations were based on the hexagonal cell with $a = 3.000$ and $c = 16.410$ Å. Within the space group

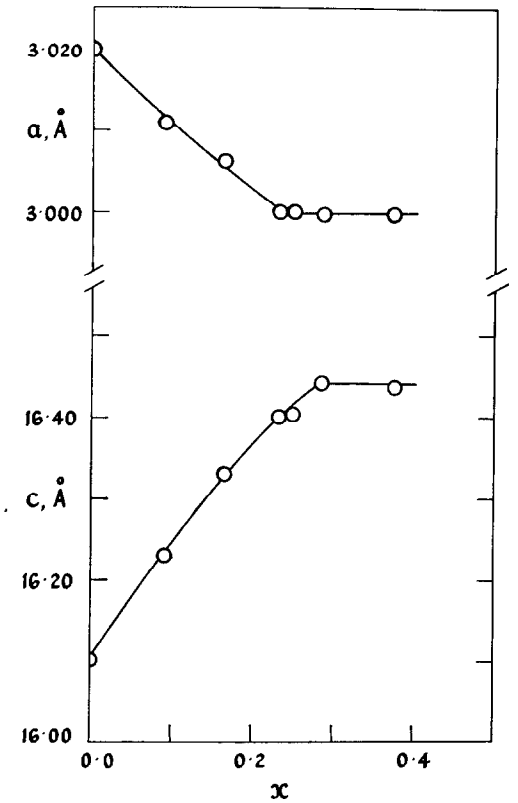

FIG. 1. Lattice parameters of $Na_{1-x}Fe_{1-x}Ti_xO_2$ as a function of $NaFeO_2$:TiO_2 ratio.

TABLE I

LATTICE PARAMETERS FOR LIMITING COMPOSITIONS

Compound	Lattice parameter (Å)[a] $x = 0$	$x = x_{limit}$	Limit of x
$Na_{1-x}Fe_{1-x}Ti_xO_2$	$a = 3.020(3)$ $c = 16.10(1)$	$a = 2.996(3)$ $c = 16.40(1)$	0.28
$K_{1-x}Al_{1-x}Ti_xO_2$	$a = 7.724(5)$	$a = 7.820(5)$	0.25
$K_{1-x}Fe_{1-x}Ti_xO_2$	$a = 7.954(5)$	$a = 7.993(5)$	0.20
$K_{1-x}Al_{1-x}Si_xO_2$	$a = 7.724(5)$	$a = 7.702(8)$ $c = 7.646(8)$	0.20

[a] Numbers in parentheses represent three standard deviations, e.g. 3.020 ± 0.003.

$R\bar{3}m$ (*1*), sodium atoms with a fractional occupancy of 0.75 were placed at the origin, with (0.75Fe + 0.25Ti) randomized in point position (3*b*) at $00\frac{1}{2}$. Oxygen was placed at $00z$ in (6*c*), with an initial value of z of 0.250. After several cycles of least-squares refinement, a final value of z of 0.2309 ± 0.0021 was obtained, with $R_{F_0} = 5.0\%$. Attempts to allow a fractional occupancy for the Fe, Ti sites, with incorporation of Fe or Ti in the Na layers, gave greatly increased values of R_{F_0}. Observed and calculated powder intensity data, for which $R_{I_0} = 6.9\%$, are shown in Table II.

TABLE II

X-RAY POWDER DIFFRACTION PATTERN OF $Na_{0.75}Fe_{0.75}Ti_{0.25}O_2$[a]; Cu K_{α_1}, KCl INTERNAL STANDARD

hkl	$\sin^2\theta_{obsd}$	$\sin^2\theta_{calcd}$	I_{obsd}	I^b_{calcd}
003	0.01980	0.01985	274	280
006	0.07930	0.07938	50	39
101	0.09012	0.09008	56	51
012	0.09657	0.09669	70	65
104	0.12316	0.12315	324	337
107	0.19604	0.19592	54	47
018	0.22914	0.22899	86	83
110	0.26380	0.26361	83	92
113	0.28356	0.28346	39	33
1.0.10	0.30842	0.30837	23	22
116	0.34309	0.34299	24	28
021	0.35465	0.35368	7	6
0.1.11		0.35468	17	16
202	0.36009	0.36030	9	11
024	0.38676	0.38676	33	38
208	0.49258	0.49260	21	19
1.1.12	0.58115	0.58113	19	22

[a] $a = 3.000 \pm 0.005$, $c = 16.40 \pm 0.01$ Å.
[b] Absolute units $\times 10^{-2}$.

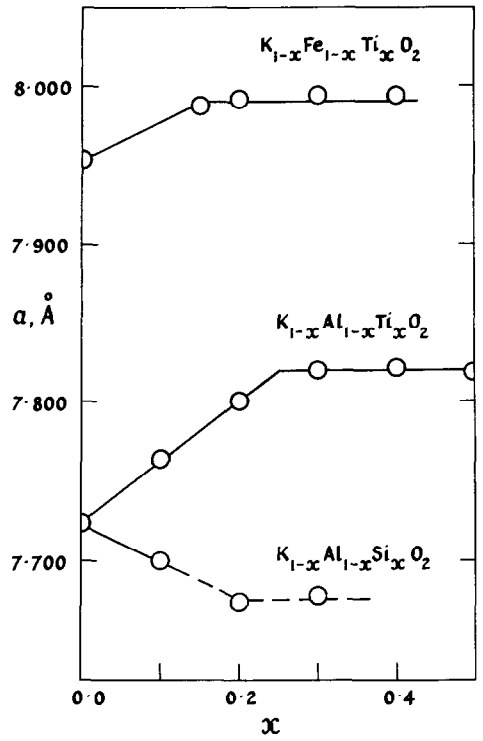

FIG. 2. Lattice parameters of $K_{1-x}Al_{1-x}Ti_xO_2$, $K_{1-x}Al_{1-x}Si_xO_2$, and $K_{1-x}Fe_{1-x}Ti_xO_2$ as a function of x. For the last compound, values beyond $x = 0.9$ are the cubic lattice parameter corresponding to the unit cell volume of the tetragonal cell.

In the $KAlO_2$–TiO_2 and $KFeO_2$–TiO_2 systems, Fig. 2, the lattice parameter changes indicated that solid solution $K_{1-x}Al_{1-x}Ti_xO_2$ with $0 < x \leqslant 0.25$ and $K_{1-x}Fe_{1-x}Ti_xO_2$ with $0 \leqslant x < 0.20$ can be formed. For each system, the limiting value of x was also inferred from the composition at which a second phase began to appear. The $K_{1-x}Fe_{1-x}Ti_xO_2$ compositions were unstable above temperatures of 800–900°C, depending on Ti content. Single-phase preparations were obtained at temperatures sufficiently low to prevent decomposition, and typically 750°C.

In the $KAlO_2$–SiO_2 system, SiO_2 entered the cristobalite-based $KAlO_2$ lattice up to the composition $K_{0.80}Al_{0.80}Si_{0.20}O_2$; beyond this composition the tridymite-based $KAlSiO_4$ structure (*11–13*) began to appear. The pseudocubic lattice parameters for $K_{1-x}Al_{1-x}Si_xO_2$ are included in Fig. 2; beyond $x = 0.90$ a pronounced splitting of the cubic lines, particularly (220), was evident, indicative of a tetragonal distortion. The powder patterns did not contain enough reflections for unambiguous indexing, but were consistent with cell parameters $a_0 = 7.702$, $c_0 = 7.646$ Å at a limiting composition $x = 0.20$.

$LiCrO_2$ (*14*), although of the α-$NaFeO_2$ type, showed little or no tolerance for accommodation of TiO_2, and no lattice parameter change could be detected when $LiCrO_2$–TiO_2 starting mixtures were reacted. Instead, the spinel $LiCrTiO_4$ (*15*) appeared, and the amount of $LiCrO_2$ progressively decreased.

Discussion

$NaFeO_2$–TiO_2 System

The α-$NaFeO_2$ structure (*1*, *4*) is derived from that of rocksalt, with an ordering of Na and Fe into layers normal to the original cube diagonal. The resulting rhombohedral distortion produces a structure which contains layers of Fe–O_6 octahedra separated by layers of Na atoms (*16*). In the hexagonal setting, $a = 3.020$ Å and $c = 16.10$ Å, Table I, all atoms lie in planes normal to the c axis. Solid solution of α-$NaFeO_2$ type compounds with others also based on the rocksalt-type lattice have been observed, e.g., between $LiCrO_2$ and MgO (*17*) and between $KPrO_2$ and K_2PrO_3 (*18*), but in such cases structural sites are not left vacant.

For $Na_{0.75}Fe_{0.75}Ti_{0.25}O_2$, the structure factor calculations showed that it is the sodium layers which contain the vacancies. As might be expected, the transition metal octahedral layers remain fully occupied. The lattice parameter plots, Fig. 1, show that the structure contracts in the a axis direction and expands along the c axis (thus increasing the rhombohedral distortion) as the sodium occupancy falls. The metal–oxygen distances for several α-$NaFeO_2$ isotypes having similar unit cell dimensions but containing metal ions of significantly different sizes (*19*) are shown in Table III. These distances show a very narrow range, indicating that in the metal–oxygen octahedral layers, the M–O separations are constrained to a relatively fixed value by the packing of the oxygen atoms. The Na–O distances show a slightly greater variability, and between α-$NaFeO_2$ and $Na_{0.75}Fe_{0.75}Ti_{0.25}O_2$ there appears to be a small but real increase in Na–O separation in addition to the increased rhombohedral distortion of the Na–O_6 octahedron.

Partial occupancy of the alkali ion layers is presumably common for the α-$NaFeO_2$ type, provided that the ions which have to randomize in the octahedral layer sites are roughly comparable in size and the alkali ion is not Li^+, which can itself randomize with Ti^{4+}, Cr^{3+}, or Fe^{3+}. In the system $NaTiO_2$–TiO_2, e.g., there should exist a composition range Na_xTiO_2–TiO_2 with $1 \geqslant x > 0.70$ based on

TABLE III

STRUCTURAL PARAMETERS FOR SOME α-$NaFeO_2$ ISOTYPES

	a (Å) ± 0.003	c (Å) ± 0.01	V (Å)^3	Z	Na–O (Å)	M–O (Å)
$Na_{0.75}Fe_{0.75}Ti_{0.25}O_2$	3.000	16.40	127.8	0.2309(21)	2.413(18)	2.027(16)
$NaFeO_2$	3.020	16.10	127.2	0.2309[a]	2.399[a]	2.027[a]
Na_2CoTiO_4[b]	3.008	16.18	126.8	0.2314(60)	2.394(56)	2.030(56)
Na_2NiTiO_4[b]	3.010	16.09	126.2	0.2320(30)	2.379(29)	2.029(29)

[a] Assuming the same fractional atomic coordinate as for $Na_{0.75}Fe_{0.75}Ti_{0.25}O_2$.
[b] Ref. (*20*).

the $NaTiO_2$ (*21*) end member. It is also possible that sulphides and selenides with the α-$NaFeO_2$ structure can exhibit a similar fractional occupancy of the alkali ion sites when charge compensated with, for example, the disulphides of Ti, Nb, or Mo. Indeed, a wide range of occupancy for potassium in K_xTiS_2 has been observed, with the α-$NaFeO_2$ structure being retained for $1 \geqslant x > 0.28$ (*22*).

The α–β-$NaFeO_2$ transition temperature was considerably raised by incorporation of TiO_2 in the structure, being greater than 1000°C for $Na_{0.8}Fe_{0.8}Ti_{0.2}O_2$ as compared with 760°C for $NaFeO_2$ (*7*). This effect can be ascribed to the preference of Ti^{4+} for octahedral sites, as observed, e.g., in garnets (*23–25*). While it is possible that Ti^{4+} could enter the tetrahedral sites in the wurtzite-like form of β-$NaFeO_2$, at a nominal composition $Na_{0.9}Fe_{0.9}Ti_{0.1}O_2$ both α and β forms coexisted at 1000°C, and the lattice parameters of the α phase showed it to be Ti-rich with respect to the β phase.

In the pseudobinary $NaFeO_2$–TiO_2 system there are three further sodium-based phases, each of which can exhibit a range of partial occupancy of sodium ions. In each case, the crystallographic sodium sites are formed within a fully occupied framework of metal–oxygen octahedra containing randomized Fe^{3+} and Ti^{4+}. In $NaFeTiO_4$ (*9*), which is of calcium ferrite type (*26–28*), Na atoms occupy sites 3 Å apart in infinite linear tunnels, with a lower occupancy limit of 0.970 ± 0.005. In $Na_xFe_xTi_{2-x}O_4$, $0.90 \geqslant x \geqslant 0.75$ (*10*), Na atoms partially occupy double tunnels of staggered sites 3 Å apart and in the $NaFeTi_3O_8$ structure (*29–31*) isotypic with $Na_xTi_4O_8$ (*32*), the sodium atom occupancy can decrease to 0.67, giving a composition $Na_{0.67}Fe_{0.67}Ti_{3.33}O_8$ (*30*). In this structure sodium ions are contained in linear tunnels of perovskite-like sites 3.8 Å apart.

The $NaFeO_2$–TiO_2 tieline contains the only ternary oxide compounds so far known in the Na_2O–Fe_2O_3–TiO_2 system, shown in Fig. 3. Attempts to prepare other ternary oxides have so far produced only mixtures of those shown. In this system, the binary oxide compounds $Fe_2Ti_3O_9$

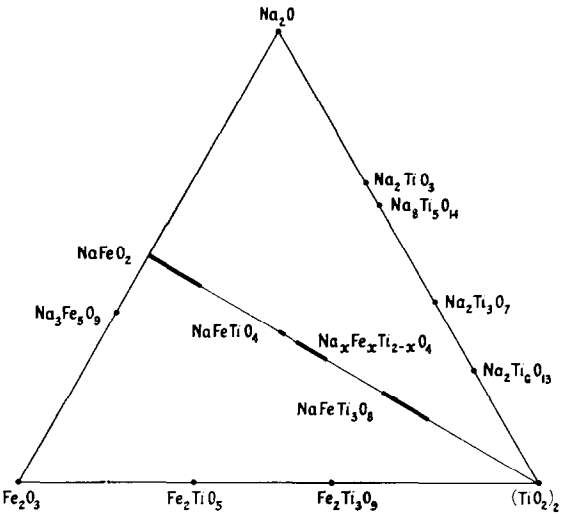

FIG. 3. The ternary oxide system Na_2O–Fe_2O_3–TiO_2. Of the compounds on the Na_2O–TiO_2 tieline only $Na_2Ti_3O_7$ (*36*) and $Na_2Ti_6O_{13}$ (*37*) have been structurally characterized. Na_2TiO_3, melting point 1030°C, has been studied as an end member of a number of phase diagrams (*38*), and is believed to be similar in structure to Na_2SnO_3 (*39*). The structure of $Na_8Ti_5O_{14}$ (*38*, *40*) is unknown. A compound $Na_4Ti_3O_8$ is also believed to have a transient existence (*41*). On the Fe_2O_3–TiO_2 tieline, $Fe_2Ti_3O_9$ (*34*) is similar to but not identical with $Cr_2Ti_2O_7$ (*42*). A naturally occurring form of $Fe_2Ti_3O_9$ (*32*) based on the ilmenite structure has also been reported with the Fe^{2+} cation layers of ilmenite replaced by layers in which Fe^{3+} ions occupy two-thirds of the original Fe^{2+} sites. The structure of Fe_2TiO_5, pseudobrookite, has long been known (*43*). On the Fe_2O_3–Na_2O tieline, $Na_3Fe_5O_9$ has been described by Romers *et al.* (*35*). The compounds on the $NaFeO_2$–TiO_2 tieline are discussed in the text.

(*33*, *34*) and $Na_3Fe_5O_9$ (*35*), have themselves been characterized only recently.

$KFeO_2$ and $KAlO_2$ with TiO_2

The structures of $KAlO_2$ and $KFeO_2$ (*2*, *44*) are based on that of β-cristobalite, the highest temperature, lowest density modification of SiO_2 (*13*, *45*). In the idealized form of this cubic structure, Si atoms occupy corners, face centers and the four $\frac{1}{4}\frac{1}{4}\frac{1}{4}$ positions of the unit cube of side 7.05 Å. Each Si is at the center of four neighbors as in the arrangement of carbon atoms in diamond, with the addition of oxygen atoms midway between silicon atoms. The real structure (*13*, *44–46*) is a distortion of this, involving the less symmetrical space group T^4 ($P2_13$). The center of the unit cube contains a large unoccupied cage site, as shown in Fig. 66 of Ref. (*13*), and in $KAlO_2$ and $KFeO_2$ this is occupied by potassium ions, with Fe or Al ions occupying the Si sites. This arrangement gives K atoms a 12-fold coordination, with bonds to two oxygen atoms of each of the Al–O_4 or Fe–O_4 tetrahedra situated at the cube faces. The oxygen coordination number is correspondingly increased from two to three. As for β-cristobalite, the real structure must involve a distortion of atoms from these ideal positions, otherwise the Al–O, Fe–O, and K–O distances would be unrealistic (*19*, *45*). However, detailed atomic coordinates have not yet been determined.

For $KAlO_2$ and $KFeO_2$, nonstoichiometry produced by inclusion of TiO_2 in the lattice extends to the compositions $K_{1-x}Al_{1-x}Ti_xO_2$ with $0 \leqslant x \leqslant 0.25$, and $K_{1-x}Fe_{1-x}Ti_xO_2$ with $0 < x < 0.20$. On the basis of the large size of potassium atoms and their position in cage-like sites in a cristobalite framework, this nonstoichiometry will certainly involve a partial occupancy of the cage sites. The required charge balance is then retained by a randomization of Al^{3+} and Ti^{4+} or Fe^{3+} and Ti^{4+} in the framework of metal–oxygen tetrahedra. Tetrahedral coordination to oxygen is unusual for Ti^{4+}, although 5-coordination in the form of square pyramids in $Ba_2TiSi_2O_8$, fresnoite (*47*), and trigonal bipyramids in $K_2Ti_2O_5$ (*48*) have been reported. However, Espinoza (*23*) has shown that in particular garnets, Ti^{4+} can replace Ga^{3+} in up to one sixth of the tetrahedral sites, and lesser amounts of Ti^{4+} in tetrahedral sites have been observed in other garnets (*24*).

Substitution of Ti^{4+} for Fe^{3+} in the tetrahedral sites of $KFeO_2$ *increases* the lattice parameter, as shown in Fig. 2, and it is of interest to try to estimate the size of the Ti–O_4 tetrahedron. For three-coordinate oxygen atoms, Si–O, Al–O, and Fe–O tetrahedral bond lengths are 1.62, 1.75, and 1.85 Å, respectively, (*19*, *49*, *50*) and a plot of unit cell volume *vs* average tetrahedral bond length (*51*) for the three compositions $K_{0.8}Al_{0.8}Si_{0.2}O_2$, $KAlO_2$, and $KFeO_2$ was found to be linear. Using this line as a basis, the change in lattice parameter as Ti^{4+} replaces Al^{3+} in $K_{1-x}Al_{1-x}Ti_xO_2$ (Fig. 2) corresponds to a tetrahedral Ti–O bond length of 1.92 Å. This is abnormally high in relation to typical Ti–O octahedral distances of 2.00 Å (*19*) and indicates that a tetrahedral Ti–O_4 configuration is not only unstable, but also relatively large. Substantial concentrations can be expected to exist only in a relatively unconstrained structure such as that of $KFeO_2$ where the framework can expand to match the tetrahedral ion size, and randomization of Ti^{4+} with Si^{4+} in tetrahedral silicate sites is unlikely. Thus in the titanium-substituted andradite garnets $Ca_3Fe_2Si_3O_{12}$ (*52*), e.g., in which up to 50% of the Si^{4+} can be replaced by Ti^{4+}, Mössbauer spectroscopy shows that an occupancy rearrangement occurs with Ti^{4+} entering octahedral sites and Fe^{3+} randomizing with Si^{4+} in the tetrahedral sites.

When further TiO_2 is added to the $KAlO_2$ and $KFeO_2$-based phases, a second phase (*53*) typified by $K_{0.75}Fe_{0.75}Ti_{1.25}O_4$ appears, and disproportionation to give this phase also occurs for $K_{1-x}Fe_{1-x}Ti_xO_4$ compositions if they are heated to too high a temperature. $K_{0.75}Fe_{0.75}Ti_{1.25}O_4$ contains puckered layers of (Fe, Ti)–O_6 octahedra, with K atoms partially occupying the sites in a structure which is related to that of $Rb_xMn_xTi_{2-x}O_4$ (*54*). As the Ti:Fe or Ti:Al ratio is further increased, the hollandite structure, in which potassium atoms are contained in linear tunnels bounded by a framework of edge-shared pairs of octahedra, (*55*) is formed. The hollandite isotype of end member composition $KAlTi_3O_8$ has an existence range down to $K_{0.75}Al_{0.75}Ti_{3.25}O_8$ (*56*), and we have observed a similar occupancy in potassium iron titanate of the hollandite form.

$KAlO_2$–SiO_2

As expected for a structure based on cristobalite, $KAlO_2$ can accommodate SiO_2 in the framework sites up to a composition $K_{1-x}Al_{1-x}Si_xO_2$ with $0 \leqslant x \leqslant 0.20$. Presumably since the Si:Al ratio is relatively low, and the lattice parameter change is linear with Si concentration, Al and Si are randomized in these sites. The decrease in unit cell volume as Si replaces Al, Fig. 2, is consistent with the unit cell volume *vs* tetrahedral bond length values observed for $KAlO_2$ and $KFeO_2$, assuming an Si–O bond length of 1.62 Å (*19*, *49*).

Tridymite, the next most dense silica polymorph,

also contains large empty sites, but only half the number of those in cristobalite. The sites lie in linear tunnels formed by rings of six tetrahedra corner joined with alternate tetrahedra pointing up and down. The compound $KAlSiO_4$, kalsilite (*12*), is based on this tridymite framework and in the $KAlO_2$–SiO_2 system, $KAlSiO_4$ was found to co-exist with $K_{0.80}Al_{0.80}Si_{0.20}O_2$ when the Si:Al ratio was increased beyond 1:4. Beyond $KAlSiO_4$ (which itself may be obtained with a potassium occupancy of less than unity) increase in Si:Al ratio leads to formation of $KAlSi_2O_6$, leucite (*13*) and finally to $KAlSi_3O_8$, sanidine. In it, as in all feldspars (*13*), the alkali ions are contained in large cage sites in the three dimensional framework of aluminosilicate tetrahedra, with one cage site to four tetrahedral sites. At very high pressures, sanidine is transformed to the hollandite form (*57*), isotypical with $KAlTi_3O_8$, while silica itself transforms to rutile form (*58*), which has no sites for additional ions.

Conclusion

The structures examined in the present paper each contain alkali ions in sites contained within a framework of coordination polyhedra formed about ions considerably smaller than sodium or potassium. Such structures appear almost universally to be able to support a nonstoichiometry based on fractional occupancy of the alkali ion sites, with a corresponding charge balance being provided within the fully occupied octahedral or tetrahedral framework. This phenomenon is not of course confined to aluminates, ferrites, or titanates, although the alkali-containing ternary titanates are a particularly rich source of such structures. It is also the basis of the marked nonstoichiometry of the various alkali-containing "bronzes" of vanadium, molybdenum, and tungsten, as well as the basis of deviations from stoichiometry in the alkali-metal aluminosilicates and of the incorporation of alkali ion impurities in the natural modifications of silica.

Acknowledgments

The authors gratefully acknowledge computer programs supplied by Mr. C. H. J. Johnson, Division of Applied Chemistry, C.S.I.R.O., and by Dr. J. J. Daly and Dr. P. J. Wheatley, Monsanto S.A., Zurich (*59*).

References

1. R. W. G. Wyckoff, "Crystal Structures," 2nd ed., Vol. 2. Wiley, New York, 1964.
2. R. Hoppe, "Mem. du Coll. Int. Cent. Nat. Rech. Sci.," *Bull. Soc. Chim. Fr., 5th ser.* 1115–1121 (1965).
3. V. I. Spitsyn, I. A. Murav'eva, L. M. Kovba, and I. I. Korchak, *Russ. J. Inorg. Chem.* **14**, 759 (1969).
4. S. Goldsztaub, *C. R. H. Acad. Sci.* **196**, 280 (1933).
5. S. Hilpert and A. Lindner, *Z. Phys. Chem. Abt. B* **22**, 395 (1933).
6. F. Bertaut and P. Blum, *C. R. H. Acad. Sci.* **239**, 429 (1954).
7. J. Théry, D. Briancon, and R. Collongues, *C. R. H. Acad. Sci.* **252**, 1475 (1961).
8. E. F. Bertaut, A. Delapalme, and G. Bassi, *C. R. H. Acad. Sci.* **257**, 421 (1963).
9. A. F. Reid, A. D. Wadsley, and M. J. Sienko, *Inorg. Chem.* **7**, 112 (1968).
10. W. G. Mumme and A. F. Reid, *Acta Crystallogr. Sect. B* **24**, 625 (1968).
11. G. F. Claringbull and F. A. Bannister, *Acta Crystallogr.* **1**, 42 (1948).
12. A. J. Perotta and J. V. Smith, *Acta Crystallogr.* **16**, A13 (1963).
12. A. J. Perotta and J. V. Smith, *Acta Crystallogr. Sect. A* **16**, A13 (1963).
13. L. Bragg and G. F. Claringbull, "Crystal Structures of Minerals," Bell, London, 1965.
14. W. Rüdorff and H. Becker, *Z. Naturforsch.* **96**, 614 (1954).
15. E. Kordes and E. Röttig, *Z. Anorg. Allg. Chem.* **263**, 34 (1951).
16. A. F. Reid and A. E. Ringwood, *Inorg. Chem.* **7**, 443 (1968).
17. E. Kordes and J. Petzoldt, *Z. Anorg. Allg. Chem.* **335**, 138 (1965).
18. R. Clos, M. Devalette, C. Fouassier and P. Hagenmuller, *Mater. Res. Bull.* **5**, 179 (1970).
19. R. D. Shannon and C. T. Prewitt, *Acta Crystallogr. Sect. B* **25**, 925 (1969).
20. W. G. Mumme, A. F. Reid, and C. Li, to be published.
21. P. Hagenmuller, A. Lecerf, and M. Onillon, *C. R. H. Acad. Sci.* **255**, 928 (1962).
22. M. Danot, A. LeBlanc and J. Rouxel, *Bull. Soc. Chim. Fr.*, 2670 (1969).
23. G. P. Espinosa, *Inorg. Chem.* **3**, 848 (1964).
24. J. Ito and C. Frondel, *Amer. Mineral.* **52**, 773 (1967).
25. S. Geller, *Z. Kristallogr., Kristallgeometrie, Kristallphys., Kristallchem.* **125**, 1 (1967).
26. P. M. Hill, H. S. Peiser and J. R. Rait, *Acta Crystallogr.* **9**, 981 (1956).
27. E. F. Bertaut, P. Blum, and G. Magnano, *Bull. Soc. Fr. Mineral. Cristallogr.* **129**, 536 (1956).
28. B. F. Decker and J. S. Kasper, *Acta Crystallogr.* **10**, 332 (1957).
29. A. D. Wadsley, *Z. Kristallogr. Kristallgeometrie, Kristallphys. Kristallchem.* **120**, 398 (1964).
30. G. Bayer and W. Hoffmann, *Z. Kristallogr. Kristallgeometrie, Kristallophys., Kristallchem.* **121**, 1 (1965).
31. A. F. Reid and M. J. Sienko, *Inorg. Chem.* **6**, 321 (1967).
32. S. Andersson and A. D. Wadsley, *Acta Crystallogr.* **15**, 201 (1962).

33. G. TEUFER AND A. K. TEMPLE, *Nature (London)* **211**, 179 (1966).
34. I. E. GREY, W. G. MUMME, AND A. F. REID, in press.
35. C. ROMERS, C. J. M. ROOYMANS, AND R. A. G. DE GRAAF, *Acta Crystallogr.* **22**, 760 (1967).
36. S. ANDERSSON AND A. D. WADSLEY, *Acta Crystallogr.* **14**, 1245 (1961).
37. S. ANDERSSON AND A. D. WADSLEY, *Acta Crystallogr.* **15**, 194 (1962).
38. A. M. LEVIN, C. R. ROBBINS, AND H. F. MCMURDIE, "Phase Diagrams for Ceramists," 1969 Supplement, American Ceramic Society, 1969.
39. G. LANG, *Z. Anorg. Allg. Chem.* **276**, 77 (1954).
40. I. N. BELYAEV AND A. G. BELYAEVA, *Russ. J. Inorg. Chem.* **10**, 252 (1965).
41. E. K. BELYAEV, N. M. PANASENKO, AND E. V. LINNIK, *Russ. J. Inorg. Chem.* **15**, 336 (1970).
42. M. HAMELIN, *Bull. Soc. Chim. Fr.*, 1421 (1957).
43. L. PAULING, *Z. Kristallogr. Kristallgeometrie, Kristallphys. Kristallchem.* **75**, 88 (1930).
44. T. F. W. BARTH, *J. Chem. Phys.* **3**, 323 (1933).
45. R. W. G. WYKOFF, "Crystal Structures," 2nd ed., Vol. 1, Wiley, New York, 1963.
46. R. B. SOSMAN, "The Phases of Silica," Rutgers Univ. Press, New Brunswick, N.J., 1965.
47. P. B. MOORE AND S. J. LOUISNATHAN, *Z. Kristallogr. Kristallgeometrie, Kristallphys. Kristallchem.* **130**, 438 (1969).
48. S. ANDERSSON AND A. D. WADSLEY, *Acta Chem. Scand.* **15**, 663 (1961).
49. G. E. BROWN AND G. V. GIBBS, *Amer. Mineral.* **54**, 1528 (1969).
50. J. B. JONES, *Acta Crystallogr. Sect. B* **24**, 355 (1968).
51. R. D. SHANNON AND C. T. PREWITT, *J. Inorg. Nucl. Chem.* **32**, 1427 (1970).
52. H. G. HUCKENHOLZ, *Amer. J. Sci.* **267A**, 209 (1969); and private communication by H. G. Huckenholz.
53. J. A. WATTS, A. F. REID, AND W. G. MUMME, in press.
54. A. F. REID, W. G. MUMME, AND A. D. WADSLEY, *Acta Crystallogr. Sect. B* **24**, 1228 (1968).
55. A. BYSTROM AND A. M. BYSTROM, *Acta Crystallogr.* **3**, 146 (1950).
56. G. BAYER AND W. HOFFMANN, *Amer. Min.* **51**, 511 (1966).
57. A. E. RINGWOOD, A. F. REID, AND A. D. WADSLEY, *Acta Crystallogr.* **23**, 1093 (1967).
58. S. M. STISHOV AND N. V. BELOV, *Dokl. Akad. Nauk. SSR* **143**, 951 (1962).
59. J. J. DALY, F. S. STEPHENS, AND P. J. WHEATLEY, Monsanto Research S.A., Final Report No. 52, 1963.